

# Nonlinear dynamics, granular media and dynamic earthquake triggering

Paul A. Johnson<sup>1\*</sup> & Xiaoping Jia<sup>2\*</sup>

The 1992 magnitude 7.3 Landers earthquake triggered an exceptional number of additional earthquakes within California and as far north as Yellowstone and Montana<sup>1–3</sup>. Since this observation, other large earthquakes have been shown to induce dynamic triggering at remote distances—for example, after the 1999 magnitude 7.1 Hector Mine<sup>1</sup> and the 2002 magnitude 7.9 Denali<sup>4</sup> earthquakes—and in the near-field as aftershocks<sup>5</sup>. The physical origin of dynamic triggering, however, remains one of the least understood aspects of earthquake nucleation<sup>1–5</sup>. The dynamic strain amplitudes from a large earthquake are exceedingly small once the waves have propagated more than several fault radii. For example, a strain wave amplitude of  $10^{-6}$  and wavelength 1 m corresponds to a displacement amplitude of about  $10^{-7}$  m. Here we show that the dynamic, elastic-nonlinear behaviour of fault gouge perturbed by a seismic wave may trigger earthquakes, even with such small strains. We base our hypothesis on recent laboratory dynamic experiments conducted in granular media, a fault gouge surrogate<sup>6,7</sup>. From these we infer that, if the fault is weak<sup>8–10</sup>, seismic waves cause the fault core modulus to decrease abruptly and weaken further. If the fault is already near failure, this process could therefore induce fault slip.

Several dynamic triggering mechanisms have been proposed, based primarily on fluid-mechanical interaction in the fault gouge (rock that has been highly fractured and ‘worked’ by the adjacent crustal blocks into a granular state<sup>2,6,7</sup>), because remote triggering appears more commonly in geothermal areas<sup>3</sup>. Proposed mechanisms include increased pore pressure associated with the following: the compaction of saturated fault gouge (liquefaction), leading to failure<sup>3</sup>; cyclic fatigue of gouge from the oscillatory wave<sup>11</sup>; and a ‘sub-critical crack growth’ mechanism in which, at crack tips in wet rocks, chemical reactions are accelerated by the wave stresses, leading to failure<sup>12,13</sup>. It was reported recently that co-seismic release of CO<sub>2</sub> overpressure from a deep source (presumably rare) was responsible for the triggering of activity related to two large events in northern Italy<sup>14</sup>. It has also been shown that triggering takes place in regions not associated with geothermal activity<sup>15–19</sup>. Thus, one or more mechanisms must exist that can explain triggering in dry or both wet and dry conditions. In short, there is much speculation about the mechanism, but experimental and field validation is lacking.

We suspect that dynamic elastic nonlinearity of fault gouge might have a function in triggering because we have observed temporary decrease in modulus (material softening) in the laboratory in a variety of rock types under the influence of wave excitation at seismic strains ( $10^{-6}$  to  $10^{-4}$ ) (ref. 20). Bearing this in mind, we set out to study material softening in granular media in the laboratory, and to understand its relationship to material weakening, a necessary ingredient in dynamic triggering. A schematic diagram of the experimental setup is shown in Fig. 1. The granular medium is

composed of glass beads of diameter  $d = 0.6–0.8$  mm, poured into a duralumin cylinder of diameter  $D = 30$  mm and filled to a height of  $L = 18.5$  mm. The container is closed with two fitted pistons (piezoelectric transducers) and a normal load corresponding to effective pressure  $P$  (effective pressure = confining pressure minus pore pressure, and the pore pressure is 1 atm (0.101 MPa)) ranging from 0.07 to 0.3 MPa is applied to the granular sample across the top piston. Before the acoustic measurements, ten cycles of loading and unloading are performed to consolidate the sample. The volume fraction of glass beads thus obtained is found to be  $0.63 \pm 0.01$ . The bead packing is then held under stress for 12 h so that the healing process of asperity contact between the grains, known as ‘aging’<sup>7,21</sup>, comes to equilibrium.

In the Earth, the fault core may be impacted by all conceivable wave types. Here we limit our studies to compressional P waves (actually Young-mode waves) to discern whether the general effect of modulus reduction takes place. Wave velocities in the glass bead pack were measured with the application of resonance and travelling wave methods. Because of self-amplification, resonance provides the most sensitive means by which to interrogate elastic nonlinear behaviour quantitatively (see Methods). Figure 2a shows resonance curves in the glass bead pack under 0.11 MPa effective pressure. The graph shows a plot of detected amplitude against frequency at progressively increasing input voltages, normalized by the input voltage. As input voltage is increased, the resonance frequency  $f_r$  decreases, corresponding to a decrease in velocity and modulus. The resonance peak

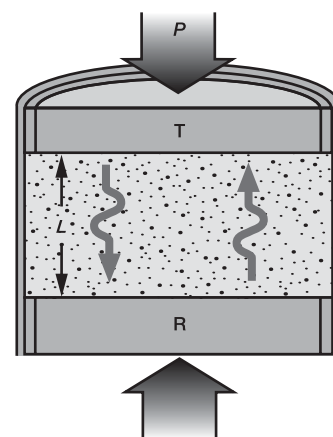


**Figure 1** | Diagram of the set-up for conducting resonance and pulse-mode experiments in the glass bead pack under applied pressure  $P$ . T and R denote the piezoelectric transmitter and the receiver, respectively, and  $L$  is the sample thickness.

<sup>1</sup>Geophysics Group EES-11, Los Alamos National Laboratory of the University of California, MS D443, Los Alamos, New Mexico 87545, USA. <sup>2</sup>Laboratoire de Physique des Matériaux Divisés et des Interfaces, Université de Marne-la-Vallée, CNRS UMR 8108, Cité Descartes, 77454 Marne la Vallée cedex 2, France.

\*These authors contributed equally to this work.

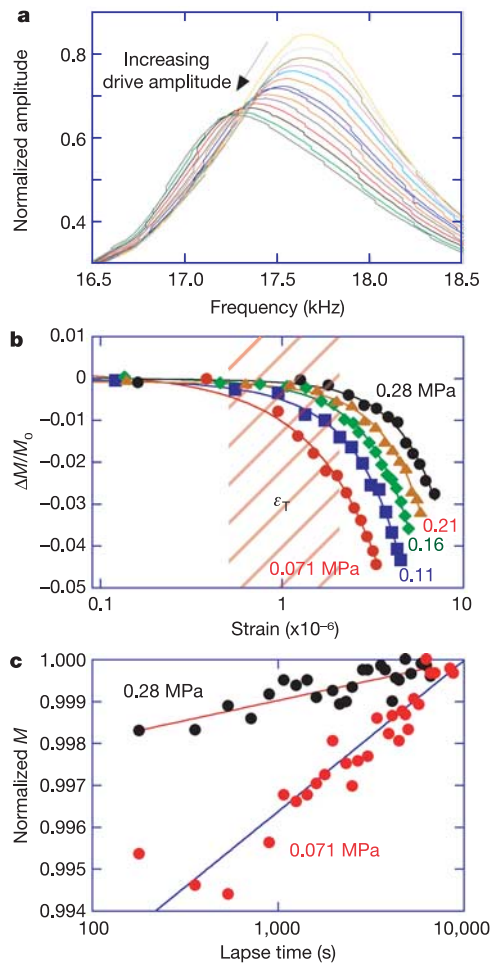


**Figure 2 | Material softening due to nonlinear dynamics under resonance conditions.** **a**, Resonance curves of the fundamental P-wave mode with increasing input amplitude measured at the detector R (see Methods). **b**, The change in normalized modulus  $\Delta M/M_0 = (M - M_0)/M_0$  with detected strain at five effective pressures as noted.  $M$  is the modulus as a function of amplitude, and  $M_0$  is the low-amplitude (linear) modulus. **c**, Slow dynamics recovery of the modulus under two different effective pressures, showing the recovery of the modulus with lapse time. The modulus is normalized to its rest, equilibrium value.

broadening and amplitude decrease is an indication of significant, simultaneous nonlinear dissipation<sup>22</sup>. The change in  $f_r$  of about 2.6% corresponds to a decrease in Young modulus of about 5.2% over a strain amplitude range of  $10^{-7}$  to  $5 \times 10^{-6}$ . For comparison, strains measured from seismic waves at hundreds of kilometres from a moderate sized earthquake are of order  $10^{-7}$  to  $10^{-6}$ , depending on the distance travelled and the source radiation pattern<sup>1,3,4</sup>.

To explore the influence of effective pressure on the nonlinear response, our experimental procedure is repeated at five progressively increasing pressures, as shown in Fig. 2b. Modulus softening diminishes progressively as the pressure is increased, meaning that the system elastic nonlinearity decreases with increasing pressure. The decrease in normalized modulus change  $\Delta M/M_0$  ( $\sim 2\Delta f/f_r = 2\Delta V/V_0$ , where  $M_0$  is the linear, equilibrium modulus) ranges from about 4.8% to 3% between 0.071 and 0.28 MPa effective pressure, respectively, for strains ranging from  $10^{-7}$  to  $7 \times 10^{-6}$ . Thus, in the fault core, we may expect the same behaviour if the fault is weak and/or the effective pressure is low. There is evidence that the effective pressure in some fault cores can be very low<sup>8,9</sup> from high fluid pressure, or that tectonically induced weakness may exist<sup>10</sup> in others. Furthermore, we see that there exists an approximate strain 'threshold'  $\varepsilon_T$  below which the granular material behaves as a linear

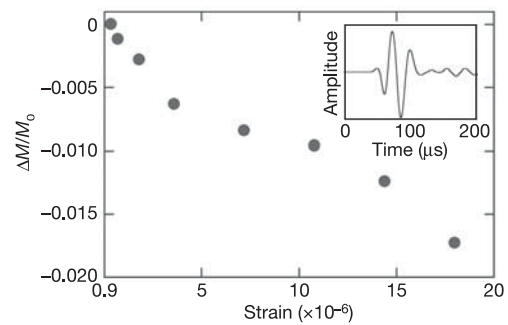


**Figure 3 | Relative decrease in modulus with input amplitude in the travelling-wave experiment for the glass-bead pack under an effective pressure of 0.11 MPa.** The source signal is a one-cycle sinusoidal pulse at 50 kHz (inset), input at progressively larger input levels from low amplitude (linear regime) to high amplitude (nonlinear regime). The actual wave velocity of about  $630 \text{ m s}^{-1}$  and modulus obtained in the linear regime (low amplitude) are identical to those obtained in the resonance experiments shown in Fig. 2. The inset shows an example of a detected waveform.

elastic medium (cross-hatched region in Fig. 2b); the resonance frequency and consequently the modulus are independent of strain amplitude below  $\varepsilon_T$ .  $\varepsilon_T$  increases progressively with effective pressure but is of order  $10^{-6}$  over the effective pressures studied. We argue below that  $\varepsilon_T$  is significant in triggering.

We find that the material softening has memory, termed 'slow dynamics'<sup>23</sup>, meaning that the modulus slowly returns to equilibrium over several hours or even days after the wave energy has disappeared. Figure 2c shows the recovery of modulus under two different pressures after excitation at large wave strains (about  $5 \times 10^{-6}$ ); the plot of  $\Delta M/M_0$  against lapse time follows a logarithmic law (although with significant scatter). The dynamic-induced modulus change and successive recovery depend strongly on the effective pressure; for example,  $\Delta M/M_0$  after  $10^4$  seconds (2.8 h) is about 1% under equilibrium for 0.071 MPa and 0.2% under equilibrium for 0.28 MPa (Fig. 2c). The actual duration of the slow dynamics in granular media is as yet only partly quantified because thermal effects in the laboratory that affect material velocity ultimately contaminate the observation, especially late in recovery time. At a minimum, the material is left in a softened state for hours after wave excitation. We argue below that slow dynamics could also have a function in triggering. Logarithmic recovery of slow dynamics has been observed in materials including rock<sup>22,23</sup> and in the ageing of granular materials that are disturbed by shear motion<sup>24</sup> or stirring. However, in the present experiment no visible rearrangement of grains was induced by acoustic vibration. These processes may be due to frictional healing of asperity contact between grains, weakened or broken during the wave vibration<sup>7</sup>.

We now examine the dynamical nonlinear response of the granular material with travelling-wave experiments, analogous to field circumstances in which a seismic wave impinges on a fault. We employed the same experimental set-up as that described in Fig. 1. Figure 3 shows that the modulus softening is immediate on perturbation by the wave pulse and also exhibits dependence on the wave amplitude. In comparison with the resonance studies (Fig. 2b), the dynamically induced reduction in modulus is less pronounced for an equivalent strain amplitude: the magnitude of modulus softening also depends on wave duration. This phenomenon, known as 'conditioning', is observed in other systems including rocks, some ceramics and damaged solids<sup>22,23</sup>. Here, conditioning more than doubles the modulus change for the equivalent strain amplitude in resonance. Nonetheless, the travelling wave measurements indicate that at a microstrain, elastic nonlinear effects appear and modulus reduction is initiated (always with the caveat that the core is weak). Finally, we note that very recent field experiments in granular media<sup>25</sup>

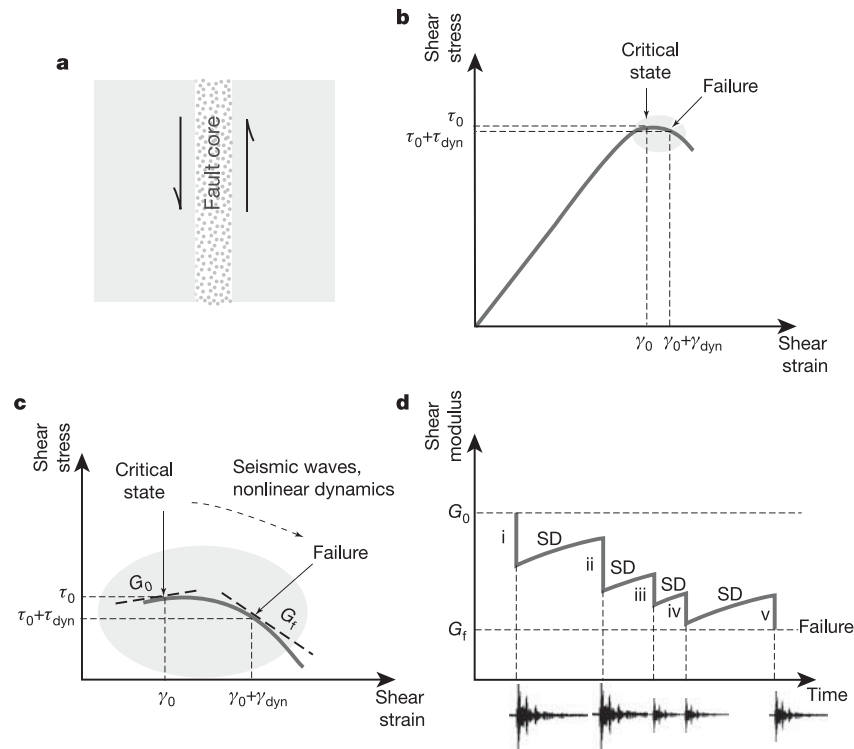


**Figure 4 | Failure model: how wave nonlinear dynamics forces a fault system that is in a critical, jammed state to failure by softening and weakening the gouge.** **a**, The physical system of a fault core and the surrounding fault blocks. **b**, The shear-stress ( $\tau$ ) versus shear-strain ( $\gamma$ )

fault-core response. **c**, Expanded view of the region of instability noted by the ellipse in **b**. See Methods for definition of variables and details. **d**, The influence of slow dynamics (SD) where successive seismic waves drive the fault core to failure. See Methods for a full description of the process.

at seismic frequencies show all of the behaviours described in the present laboratory experiments.

We believe the physical mechanism responsible for the modulus softening of the granular material is related to the nonlinear frictional properties at the contacts between the grains. A very simple phenomenological model that captures the general nature of the material elasticity can be described as follows. At a given effective stress  $\sigma_0$ , the dynamic stress  $\sigma_{\text{dyn}}$  is<sup>20,26</sup>

$$\sigma_{\text{dyn}} = M \varepsilon_{\text{dyn}} \left( 1 + \beta \varepsilon_{\text{dyn}} + \delta \varepsilon_{\text{dyn}}^2 + \dots \right) \quad (1)$$

where  $\varepsilon_{\text{dyn}}$  is the dynamic strain,  $M$  is the modulus, and  $\beta$  and  $\delta$  are the first-order and second-order dynamic nonlinear parameters that describe the shape of the curves in Fig. 2b (a more comprehensive relation is hysteretic but will not affect the proposed model of triggering). It can be inferred from Fig. 2b that  $\beta$  and  $\delta$  vary with the effective pressure and thus with  $\sigma_0$ . From contact mechanics<sup>27</sup>  $\beta$  and  $\delta$  are proportional to  $1/\varepsilon_0$  and  $1/\varepsilon_0^2$ , respectively. For  $\varepsilon_0 = 1.3 \times 10^{-4}$ , corresponding to an applied pressure of about 0.11 MPa,  $\beta$  and  $\delta$  are order of  $-7.7 \times 10^5$  and  $-5.9 \times 10^7$ , respectively (for comparison,  $|\beta| < 10$  for steel). Slow dynamics and conditioning related to the healing process of grain-grain contacts can also be included phenomenologically in this model, in which  $M$  has a log(time) dependence.

Taking the above equation of state, we relate the material softening to weakening, by applying logic resembling that of Rice and Rudnicki<sup>28,29</sup>. We consider the soft fault core surrounded by competent fault blocks in Fig. 4a and the effect of a seismic wave impinging on the system that is in a critical state, near failure (Fig. 4b). To produce significant material softening and simultaneous weakening, taking the fault gouge through the instability and failure (Fig. 4c), the laboratory experiments described here show that the perturbing wave strain must be at least about  $10^{-6}$ . This is shown by the cross-hatched region in Fig. 2b. We suggest that this is why most

seismic waves, even from large earthquakes, do not cause triggering (except in what is traditionally deemed the aftershock zone<sup>5,30</sup>)—their strain amplitudes tend to be  $10^{-7}$  to  $10^{-6}$  at regional distances<sup>1,3,4</sup>. Only large earthquakes that focus sufficiently large high amplitudes of several microstrains, such as the Denali and Landers events, cause triggering beyond the aftershock zone<sup>30</sup>. In these cases, the fault core at equilibrium must be in a critical state, in which it can be taken through instability to failure by the perturbation of the seismic wave. Equivalently, we may also interpret triggering as the onset of sliding of the fault, resulting from an abrupt decrease in the shear strength of the granular gouge by break or loss of contact due to strong vibration<sup>7</sup>. Figure 4d describes how slow dynamics could also have a function in inducing delayed triggering in the situation where successive seismic waves impinge on the fault from a foreshock–mainshock–aftershock sequence.

Thus, our laboratory experiments in combination with the softening-to-weakening model presented here indicate that dynamic elastic nonlinearity of the fault core—the gouge—offers an explanation for the occurrence of dynamic triggering in response to seismic waves. Slow dynamics might be responsible for delayed triggering. The necessary physical characteristics for this triggering mechanism require three factors: first, a weak fault (or one with low effective pressure); second, a fault in a critical state; and third, dynamic strain amplitudes greater than about  $10^{-6}$ .

## METHODS

**Resonance experiment.** To optimize the propagation of coherent P waves, large piezoelectric transducers of diameter  $D = 30$  mm placed in direct contact with the glass beads are used as the excitation source and receiver<sup>21</sup> (Fig. 1). The vibration displacement  $u_{\text{dyn}}$  of piezoelectric transducers is calibrated by an optical interferometer measuring displacement directly on the transducer face, and calculating dynamic strain  $\varepsilon_{\text{dyn}}$  according to  $\varepsilon_{\text{dyn}} = du_{\text{dyn}}/dx = 2\pi u_{\text{dyn}}/\lambda$ , where  $\lambda$  is the wavelength. We measure resonance in our confined, granular samples over a frequency-sweep interval that contains the fundamental modes.

At each frequency interval in the sweep, the frequency is held fixed until the wave amplitude reaches steady-state conditions. We then extract the time-averaged amplitude at each frequency in the sweep to construct a resonance curve composed of frequency versus amplitude. Curves are obtained at progressively increasing amplitude levels, as seen in Fig. 2a. The resonance frequency shift measured at the curve peak plotted against its detected strain amplitude is then used to characterize the material nonlinearity (Fig. 2b). This is accomplished by monitoring the resonance-induced reduction of effective wave velocity or elastic modulus, according to the relationship  $f_r = V/2L$ , obtained in a resonator of thickness  $L$  with rigid boundary conditions, where  $f_r$  is the resonance peak frequency and  $V$  the P-wave velocity, and also  $V = (M/\rho)^{1/2}$  where  $M$  is the Young modulus and  $\rho$  is the material density. The granular density of our glass beads stressed by means of a jackscrew arrangement undergoes expansion during the resonance experiments; at 0.11 MPa, for instance, the effective pressure  $P$  is observed to increase by about 3%, which would correspond to an increase in modulus of  $\Delta M/M_0 \approx 1\%$  according to the hertzian contact elasticity<sup>27</sup>. This observation, probably arising from a dilatancy-like effect in our dense glass bead packs, implies that the decrease in modulus induced by acoustic vibration might be even stronger than that illustrated in Fig. 2b.

**Slow dynamics experiment.** In the slow dynamics measurement, the equilibrium, elastically linear modulus of the sample is first measured by applying a low-amplitude strain (of order  $10^{-7}$ ) step-sweep and constructing a resonance curve as described above. The amplitude at the resonance peak is recorded. The sample is then vibrated at fixed frequency near the resonance at a large strain amplitude, corresponding to the maximum amplitudes shown in Fig. 2b, for 7 min to induce material softening. Immediately on termination of the high-amplitude excitation, the step-sweep measurement recommences at very low strain to probe the recovery of the resonant peak frequency (modulus) as a function of elapsed time, as shown in Fig. 2c.

**Fault core softening, weakening and triggering.** The fault core's mechanical response is controlled by the gouge itself and/or roughness on the blocks, presumed granular in nature, shown in Fig. 4a. The stress-strain tensor of the fault core is

$$\varepsilon_{ij} = M_{ijkl}^{-1} \sigma_{kl} \quad (2)$$

The fault core fails in shear, so we consider single shear-stress ( $\tau$ ) and shear-strain ( $\gamma$ ) components of  $\sigma_{ij}$  and  $\varepsilon_{ij}$ ,  $i \neq j$ , respectively. The shear modulus  $G = \partial\tau/\partial\gamma$  is assumed much smaller in the core than the surrounding blocks. As shown in Fig. 4b and its zoom (indicated by the ellipse) in Fig. 4c, the fault core is at equilibrium because of the ambient stress field, but in a critical state near failure as denoted by the shear stress and strains  $\tau_0$  and  $\gamma_0$ , where

$$\tau_0 = G_0 \gamma_0 \quad (3)$$

and the core modulus is  $G_0$ . The total stress  $\tau_{tr}$  is the sum of the equilibrium stress  $\tau_0$  and the contribution from the transient seismic wave  $\tau_{dyn}$ ,

$$\tau_{tr} = \tau_0 + \tau_{dyn} \quad (4)$$

where

$$\tau_{dyn} = G_0 \gamma_{dyn} \left( 1 + \beta \gamma_{dyn} + \delta \gamma_{dyn}^2 + \dots \right) \quad (5)$$

from equation (1). Substitution of equation (3) and equation (4) into equation (5) yields

$$\tau_{tr} = G_0 \left[ \gamma_0 + \gamma_{dyn} \left( 1 + \beta \gamma_{dyn} + \delta \gamma_{dyn}^2 + \dots \right) \right] \quad (6)$$

If the dynamic strain is zero, the equation reverts to equation (3). Thus, when  $\gamma_{dyn}$  is at a strain amplitude (more than about  $10^{-6}$ ) to cause sufficient modulus reduction, equation (6) shows how the core may quickly go from a critical state to failure. The above model differs markedly from the classical Rice–Rudnicki<sup>28,29</sup> model in that the behaviour of the fault core perturbed by a seismic wave drives the system rather than the static shear stress of the surrounding fault blocks.

**Delayed triggering.** Figure 4d shows the influence of slow dynamics (SD) where successive seismic waves drive the fault core to failure. In the case where the first wave impinging on the fault core does not cause failure, there is nonetheless a decrease in modulus from equilibrium  $G_0$  denoted by  $i$ . The core modulus begins the SD recovery towards equilibrium (SD) but does not reach it. A successive seismic wave drives the modulus even lower (ii) and the SD recommences. With successive seismic waves,  $G(t)$  ratchets progressively downwards (iii–v), recovering to some extent between seismic waves, and so on, until one wave drives the system to failure (v). Here the modulus can be described by

$$G(t_i) = G_0 \left( 1 + 2\beta \gamma_{dyn} + 3\delta \gamma_{dyn}^2 \right) \quad (7)$$

where  $G(t_i)$  is a function of  $\log(\text{time})$  after each successive event.

Received 1 February; accepted 11 July 2005.

- Gomberg, J., Reasenberg, P. A., Bodin, P. & Harris, R. A. Earthquake triggering by seismic waves following the Landers and Hector Mine earthquakes. *Nature* **411**, 462–466 (2001).
- Scholz, C. H. *The Mechanics of Earthquakes and Faulting* 2nd edn (Cambridge Univ. Press, Cambridge, 2002).
- Hill, D. P. *et al.* Seismicity remotely triggered by the magnitude 7.3 Landers, California, earthquake. *Science* **260**, 1617–1623 (1993).
- Gomberg, J., Bodin, P., Larson, K. & Dragert, H. Earthquake nucleation by transient deformations caused by the  $M = 7.9$  Denali, Alaska, earthquake. *Nature* **427**, 621–624 (2004).
- Gomberg, J., Bodin, P. & Reasenberg, P. A. Observing earthquakes triggered in the near field by dynamic deformations. *Bull. Seismol. Soc. Am* **93**, 118–138 (2003).
- Astrom, J. A., Herrmann, H. J. & Timonen, J. Granular packings and fault zones. *Phys. Rev. Lett.* **84**, 638–641 (2000).
- Marone, C. Laboratory-derived friction laws and their application to seismic faulting. *Annu. Rev. Earth Planet. Sci.* **26**, 643–696 (1998).
- Hardebeck, J. L. & Hauksson, E. Role of fluids in faulting inferred from stress field signatures. *Science* **285**, 236–239 (1999).
- Miller, S. A. Fluid-mediated influence of adjacent thrusting on the seismic cycle at Parkfield. *Nature* **382**, 799–802 (1996).
- Hardebeck, J. L. & Hauksson, E. Crustal stress field in southern California and its implications for fault mechanics. *J. Geophys. Res.* **106**, 21859–21882 (2001).
- Gomberg, J., Beeler, N. M., Blanpied, M. L. & Bodin, P. Earthquake triggering by transient and static deformations. *J. Geophys. Res.* **103**, 24411–24426 (1998).
- Brodsky, E. E., Karakostas, V. & Kanamori, H. A new observation of dynamically triggered regional seismicity: Earthquakes in Greece following the August, 1999, Ismir, Turkey Earthquake. *Geophys. Res. Lett.* **27**, 2741–2744 (2000).
- Das, S. & Scholz, C. Off-fault aftershock clusters caused by shear stress increase? *Bull. Seismol. Soc. Am* **71**, 1669–1675 (1981).
- Miller, S. A. *et al.* Aftershocks driven by high-pressure CO<sub>2</sub> source at depth. *Nature* **427**, 724–727 (2004).
- Gomberg, J. & Bodin, P. Triggering of the Little Skull Mountain, Nevada earthquake with dynamic strains. *Bull. Seismol. Soc. Am* **84**, 844–853 (1994).
- Gomberg, J., Bodin, P. & Reasenberg, P. Observing earthquakes triggered in the near field by dynamic deformations. *Bull. Seismol. Soc. Am* **93**, 118–138 (2003).
- Hough, S. E. Triggered earthquakes and the 1811–1812 New Madrid, Central United States earthquake sequence. *Bull. Seismol. Soc. Am* **91**, 1574–1581 (2001).
- Mohamad, R. *et al.* Remote earthquake triggering along the Dead Sea Fault in Syria following the 1995 Gulf of Aqaba earthquake ( $M_s = 7.3$ ). *Seismol. Res. Lett.* **71**, 47–52 (2000).
- Singh, S. K., Anderson, J. G. & Rodriguez, M. Triggered seismicity in the Valley of Mexico from major earthquakes. *Geofis. Int.* **37**, 3–15 (1998).
- Guyer, R. A. & Johnson, P. A. The astonishing case of mesoscopic elastic nonlinearity. *Phys. Today* **52**, 30–35 (1999).
- Jia, X. Coda-like multiple scattering of elastic waves in dense granular media. *Phys. Rev. Lett.* **93**, 154303 (2004).
- Johnson, P. A. & Sutin, A. Slow dynamics and anomalous nonlinear fast dynamics in diverse solids. *J. Acoust. Soc. Am* **117**, 124–130 (2005).
- TenCate, J. & Shankland, T. J. Slow dynamics in the nonlinear elastic response of Berea sandstone. *Geophys. Res. Lett.* **23**, 3019–3022 (1996).
- Hartley, R. R. & Behringer, R. P. Logarithmic rate dependence of force networks in sheared granular materials. *Nature* **421**, 928–931 (2003).
- Pearce, F. *et al.* Nonlinear soil response induced in situ by an active source at Garner Valley. *Eos* **85** (Suppl.), Abstract S42A–04 (2004).
- Ostrovsky, L. & Johnson, P. A. Dynamic nonlinear elasticity in geomaterials. *Riv. Nuovo Cim.* **24**, 1–46 (2001).
- Johnson, K. L. *Contact Mechanics* (Cambridge Univ. Press, Cambridge, 1985).
- Rudnicki, J. W. The inception of faulting in a rock mass with a weakened zone. *J. Geophys. Res.* **82**, 844–854 (1977).
- Rice, J. & Rudnicki, J. W. Earthquake precursory effects due to pore fluid stabilization of a weakened fault zone. *J. Geophys. Res.* **84**, 2177–2184 (1979).
- Gomberg, J. & Johnson, P. A. Dynamic triggering of earthquakes. *Nature* doi:10.1038/nature04167 (this issue).

**Acknowledgements** We thank J. Gomberg, C. Marrone, P. Bodin, J. Vidale, A. Freed, R. Guyer, S. Hough, C. Scholz, P. Mills, C. Lewis, S. Meadows and J. Laurent. Funding was provided by the US Department of Energy, Office of Basic Energy Science; CNRS France and the Institute of Geophysics and Planetary Physics at Los Alamos. P.J. also acknowledges a grant from CNRS.

**Author Information** Reprints and permissions information is available at [npg.nature.com/reprintsandpermissions](http://npg.nature.com/reprintsandpermissions). The authors declare no competing financial interests. Correspondence and requests for materials should be addressed to P.J. ([paj@lanl.gov](mailto:paj@lanl.gov)).